Available online at www.sciencedirect.com
SCIENCE DIRECT®
Journal of Solid State Chemistry 177 (2004) 4251–4257
JOURNAL OF SOLID STATE CHEMISTRY
www.elsevier.com/locate/jssc

Synthesis, crystal and magnetic structure of a novel brownmillerite-type compound $Ca_2Co_{1.6}Ga_{0.4}O_5$

S.Ya. Istomin[a,*], S.V. Abdyusheva[b], G. Svensson[c], E.V. Antipov[a]

[a] Department of Chemistry, Moscow State University, 119899 Moscow, Russia
[b] Department of Materials Chemistry, Moscow State University, 119899 Moscow, Russia
[c] Department of Structural Chemistry, Stockholm University, SE-10691 Stockholm, Sweden

Received 3 June 2004; received in revised form 11 August 2004; accepted 11 August 2004

Abstract

The novel compound $Ca_2Co_{1.6}Ga_{0.4}O_5$ with brownmillerite (BM) structure has been prepared from citrates at 950 °C. The crystal structure of $Ca_2Co_{1.6}Ga_{0.4}O_5$ was refined, from neutron powder diffraction (NPD) data, in space group *Pnma*, $a = 5.3022(6)$ Å, $b = 14.884(2)$ Å, $c = 5.5276(6)$ Å, $\chi^2 = 1.798$, $R_F^2 = 0.0455$, $R_{wp} = 0.0378$ and $R_p = 0.0292$. On the basis of the NPD refinement the compound was found to be a G-type antiferromagnet (space group $Pn'm'a$) at room temperature, with the magnetic moments of cobalt atoms directed along chains of tetrahedra in the BM structure. Electron diffraction and electron microscopy studies revealed disorder in the crystallites, which can be interpreted as the presence of slabs with BM-type structure of *Pnma* and *I2mb* symmetry.

Keywords: $Ca_2Co_{1.6}Ga_{0.4}O_5$; Brownmillerites; Neutron diffraction; Electron diffraction; Structure; Antiferromagnetism

1. Introduction

Materials based on oxygen-deficient perovskite-related compounds have been attracting special attention during the last 20 years. Complex cobalt oxides with perovskite structure are of interest since they exhibit both electronic and oxide-ion conductivities and can be used as electrode materials for low- and high-temperature fuel cells or as dense membranes for the separation of oxygen from gas mixtures.

One of the most stable variants of oxygen vacancy ordering in perovskites is the brownmillerite (BM) type. The structure of BM (Fig. 1) contains layers of corner-sharing octahedra separated by layers of tetrahedra. There are three different variants of relative orientation of the chains of tetrahedra at $y = \frac{1}{4}$ and $\frac{3}{4}$ in the BM-type compounds. They can be related by an inversion centre ($\bar{1}$), as in space group *Pnma* (e.g. $Ca_2Fe_2O_5$ [1–3]) or by two-fold axis (2) as in space group *I2mb* (e.g. $Sr_2Fe_2O_5$ [4]). Random distribution of the chain orientations is observed for compounds crystallizing in space group *Imma* (e.g. $Sr_2Co_2O_5$ [5,6]). Since BM-type $Ca_2Co_2O_5$ does not exist, and the Sr analogue is stable above ~900 °C only, there have been several studies on how to stabilize the BM structure for complex cobalt oxides by suitable substitution with a trivalent cation such as Al^{3+} and Ga^{3+}. BM-type structures have indeed been obtained for $Sr_2Co_{2-x}Ga_xO_5$, $0.3 \leqslant x \leqslant 0.8$ (space group *Imma*) [7], $Sr_2Co_{2-x}Al_xO_5$, $0.3 \leqslant x \leqslant 0.5$ (space group *Imma*) [8] and $Ca_2Co_{2-x}Al_xO_5$ ($x \approx 0.75$) [9]. The latter compound represents a complex variant of the BM-type structure with long-range ordering of the chains of tetrahedra.

Some years ago we unsuccessfully tried to synthesize compounds with the BM-type structure in the Ca–Co–Ga–O system. Instead, we obtained a new $Ca_2Ga_{1.2}Co_{0.8}O_{4.8}$ compound with a large cubic cell, $a = 15.0558$ Å [10]. It was found to be very stable when prepared by conventional solid-state synthesis

*Corresponding author. Fax: +7-095-939-47-88.
E-mail address: istomin@icr.chem.msu.ru (S.Ya. Istomin).

0022-4596/$ - see front matter © 2004 Elsevier Inc. All rights reserved.
doi:10.1016/j.jssc.2004.08.018

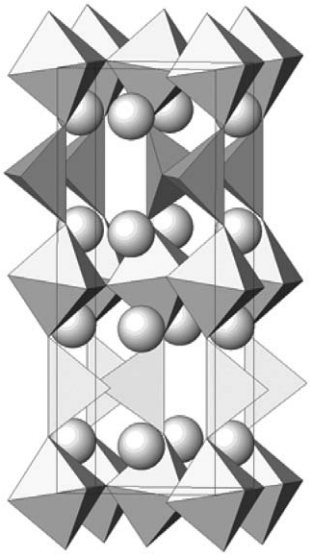

Fig. 1. Crystal structure of BM, $Ca_2(Fe, Al)_2O_5$.

techniques at high temperatures (1100–1150 °C). We have recently determined its structure [11] to be a disordered variant of $Ca_{14}Al_{10}Zn_6O_{35}$ [12]. In the present paper, we report on the successful synthesis and structural characterization of $Ca_2Co_{1.6}Ga_{0.4}O_5$ a novel BM-type compound in the Ca–Co–Ga–O system, using a synthetic route based on citrates and a low calcination temperature.

2. Experimental

Samples of $Ca_2Co_{2-x}Ga_xO_5$, $0.2 \leqslant x \leqslant 0.8$, were prepared via a citrate-based route. First Ga_2O_3 (99.999%) was dissolved in a melt of citric acid monohydrate (99.999%). To this melt, stoichiometric amounts of $CaCO_3$ (99.999%) as well as a saturated solution (minimal amount of water) of cobalt(II) nitrate hexahydrate (99.999%) was added. The resulting solution was evaporated to yield a viscous mixture, which was fired at 500 °C in air for 12 h until a black powder was obtained. The powder was pressed into pellets and annealed at 950–1100 °C for 24–96 h. Phase analysis of the samples was performed by means of XRD powder patterns recorded in a Guinier camera with focusing geometry, using Cu $K\alpha_1$ radiation and Ge as internal standard.

Room-temperature neutron powder diffraction (NPD) data were collected with the NPD instrument at the Swedish research reactor, NFL, Studsvik. The sample (~2 g) was placed in a can ($d = 8$ mm) of thin vanadium foil. Data were collected in the 2θ range 4.00–139.92° with a step length of 0.08°. The nuclear and magnetic structures were refined with the general structure analysis system suite of programs [13].

For transmission electron microscopy (TEM) studies, small amounts of the samples were crushed in *n*-butanol. A drop of this dispersion was put on a holey carbon film supported by a copper grid. Electron diffraction (ED) and high-resolution electron microscopy studies were carried out with a JEOL JEM3010 UHR microscope operated at 300 kV. EDX analyses for the determination of cation content on the same grids as studied in the TEM were performed with a JEOL JSM 880 scanning electron microscope equipped with a windowless energy-dispersive analyser (EDS) LINK *Isis*. Simulated HREM images were calculated with MacTempas [14].

Iodometric titration was used to determine the oxygen content in the as-prepared sample $Ca_2Co_{1.6}Ga_{0.4}O_5$. About 50 mg of the sample under investigation was placed in a flask containing 20 mL of a 20% water solution of KI. Several drops of concentrated HCl were then added to the solution. The flask was kept in a dark place until the entire sample had dissolved. The released elemental iodine was titrated with a standard $Na_2S_2O_3$ solution with starch added as an indicator.

3. Results and discussion

A single-phase $Ca_2Co_{1.6}Ga_{0.4}O_5$ sample was prepared by annealing in air at 950 °C for 55 h with several intermediate regrindings. All the reflections in the corresponding XRD pattern could be indexed with an *I*-centred orthorhombic unit cell, $a = 5.2988(8)$, $b = 14.885(2)$ and $c = 5.517(1)$ Å. For the compositions $x = 0.5$ and 0.6, nearly single-phase samples were obtained, the secondary phase being about 3–5 wt% cubic $Ca_2Ga_{1.2}Co_{0.8}O_{4.8}$ [10]. Only a minor non-systematic variation of the unit cell parameters of the BM phase was observed for these samples. The presence of the 1 3 1 reflection (about 3–5% intensity), indicating a primitive unit cell was observed in the XRD patterns of the $x = 0.6$ and 0.5 samples. The intensity of this reflection, which was not observed in the $x = 0.4$ sample, increased with gallium content. The oxygen content of the single-phase sample $Ca_2Co_{1.6}Ga_{0.4}O_5$ was confirmed to be stoichiometric according to the iodometric titration results. XRD showed $Ca_2Co_{2-x}Ga_xO_5$, $0.6 < x \leqslant 0.8$ to be multi-phase, with $Ca_2Ga_{1.2}Co_{0.8}O_{4.8}$ [10] and $Ca_3Ga_4O_9$ [15] as secondary phases. At lower gallium contents ($x \leqslant 0.3$) $Ca_3Co_2O_6$ appears as secondary phase. An attempt was made to prepare BM-type $Ca_2Co_{2-x}Ga_xO_5$, $0.4 \leqslant x \leqslant 0.6$ samples using conventional solid-state synthesis, including $CaCO_3$, Co_3O_4 and Ga_2O_3 as initial reagents. For $T = 900-1000$ °C large amounts of CaO, Co_3O_4 and unidentified phase together with a small quantity of BM phase were observed by means of the XRD powder patterns, even after regrinding and reheating. Increasing the temperature up to 1100–1150 °C resulted in multi-phase samples

containing CaO and the cubic-phase $Ca_2Ga_{1.2}Co_{0.8}O_{4.8}$, according to XRD. Regrinding and reheating the samples at 1100–1150 °C did not improve the result as the amount of $Ca_2Ga_{1.2}Co_{0.8}O_{4.8}$ increased. This indicates the BM phase to be unstable at high temperatures, $T > 1100$ °C. An experiment on a single-phase BM-type $Ca_2Co_{1.6}Ga_{0.4}O_5$ sample, prepared by the citrate method, confirmed this conclusion. The compound decomposes completely into $Ca_2Ga_{1.2}Co_{0.8}O_{4.8}$, CoO and CaO upon heat treatment at 1150 °C for 48 h. This explains why we did not observe the formation of a BM-type phase in our earlier study of the Ca–Ga–Co–O system at 1100–1150 °C [10].

3.1. Neutron diffraction study

The NPD experiment was performed on a newly prepared sample (~2 g) of $Ca_2Co_{1.4}Ga_{0.6}O_5$. It should be mentioned that the XRD powder patterns for this sample clearly indicate a body-centred unit cell. However, the presence of strong reflections with $h+k+l \neq 2n$ in the NPD powder pattern, for example, 1 3 1 with $I \approx 10\%$ and 1 5 1 with $I \approx 7\%$ (intensities are given in percentage to the most intensive reflection on NPD pattern), indicates that the lattice in fact is primitive. A detailed study of the reflection conditions points to the space group *Pnma*. Further study of the $Ca_2Co_{1.6}Ga_{0.4}O_5$ by ED revealed (see later) that it contains crystallites with both *I*- and *P*-centred BM structures. Discrepancy between the results of XRD and NPD can be explained by the fact that a much larger amount of the sample was used for the NPD experiment. The starting model for the structure refinement was the atomic coordinate set of BM-type $Ca_2Fe_2O_5$ [3]. There were two additional groups of reflections present in the NPD pattern, which could not be accounted for in the Rietveld refinement. The first group consisted of strong reflections that could be ascribed to a magnetic ordering in the BM-type phase. Different patterns of the magnetic moments ordering were tested. The best fit was obtained for the model analogue to $Sr_2Co_{2-x}Ga_xO_5$, $0.3 \leqslant x \leqslant 0.8$, where magnetic moments of all cobalt atoms are oriented antiferromagnetically relatively to the six nearest cobalt atoms (G-type) and directed along the chains of tetrahedra [7]. The refined magnetic moments are $1.56(6)\mu_{BM}$ for Co1 and $1.5(1)\mu_{BM}$ for Co2. The second group of reflections could be attributed to small amounts of $Ca_2Ga_{1.2}Co_{0.8}O_{4.8}$ [11] and $Ca_3Ga_4O_9$ [15]. The refined mass fractions of the phases were $Ca_2Ga_{1.2}Co_{0.8}O_{4.8}$ 0.047(2) and $Ca_3Ga_4O_9$–0.051(3). It should be noted that the refined composition of the BM-phase $Ca_2Co_{1.54(1)}Ga_{0.46(1)}O_5$ is close to the nominal composition of the single-phase sample $Ca_2Co_{1.6}Ga_{0.4}O_5$. Crystal and refinement data are given in Table 1. Atomic coordinates, occupancies and atomic displacement parameters are given in Table 2 and interatomic distances in Table 3. Observed, calculated and difference neutron diffraction intensities are given in Fig. 2.

Table 1
Crystal data for $Ca_2Co_{1.6}Ga_{0.4}O_5$

T	298 K
Space group, magnetic space group	*Pnma*, *Pn′m′a*
Lattice parameters (Å)	$a = 5.3022(6)$
	$b = 14.884(2)$
	$c = 5.5276(6)$
χ^2	1.798
R_F^2	0.0455
R_{wp}	0.0378
R_p	0.0292
Number of reflections (Bragg and magnetic), N_p	1642
Number of fitted parameters, N_f	59

Phase fractions: main phase: 0.902 (1); $Ca_2Ga_{1.2}Co_{0.8}O_{4.8}$: 0.047(2); $Ca_3Ga_4O_9$: 0.051(3) (ICSD ♯100356).

3.2. Electron diffraction and transmission electron microscopy studies

The selected-area electron diffraction (SAED) studies were performed on the same sample $Ca_2Co_{1.4}Ga_{0.6}O_5$ used for the NPD experiment. SAED confirms the sample $Ca_2Co_{1.4}Ga_{0.6}O_5$ to be polyphasic, containing the cubic-phase $Ca_2Ga_{1.2}Co_{0.8}O_{4.8}$ [10] and the hexagonal-phase $Ca_3Ga_4O_9$ in addition to the main phase, BM-type $Ca_2Co_{1.6}Ga_{0.4}O_5$. The presence of reflections like $hkl \rightarrow h+k+l \neq 2n$ confirm that the space group *Pnma* gives a better description of the crystal symmetry than *Imma* or *I2mb*, which are frequently found for the BM-type structure. The situation is somewhat

Table 2
Atomic coordinates, occupancies of the positions and atomic displacement parameters for $Ca_2Co_{1.6}Ga_{0.4}O_5$

Atom	Wy. site.	*x*	*y*	*z*	$U_{iso} \times 100/Å^2$	Magnetic moment per Co atom	Occ.
Ca	8*d*	0.494(1)	0.1091(2)	0.0224(7)	0.7(1)		1
Co1/Ga1	4*a*	0	0	0	0.0(1)	1.56(6)	0.997(8)/0.003(8)
Co2/Ga2	4*c*	0.456(1)	0.25	0.567(1)	0.9(1)	1.5(1)	0.54(1)/0.46(1)
O1	8*d*	0.251(1)	−0.0140(2)	0.2374(7)	0.76(8)		1
O2	8*d*	0.0175(8)	0.1418(2)	0.0689(4)	0.76(7)		1
O3	4*c*	0.0981(1)	0.25	0.6218(9)	1.7(2)		1

complicated, however, because streaking was always observed in the SAED patterns, indicating disorder. A number of such patterns recorded during a tilt sequence around the *b*-axis are shown in Fig. 3. In all, SAED patterns there is streaking along the *b*-axis. In addition, there is streaking along the *b*-axis between the Bragg spots of BM (marked with arrows in the images), except in the [001] zone-axis pattern (ZAP). (The lines are quite weak in some of the patterns.) In other patterns (e.g. ZAP [203] there are clear intensity maxima in the streaking indicating some ordering), a schematic interpretation of the reciprocal lattice based on these SAED patterns is shown in Fig. 4. This type of streaking has frequently been observed among BM-type compounds, and may be explained by disorder among the chains of tetrahedra [16]. A more detailed interpretation suggests a modulation along the *c*-axis related to what found in $Ca_2Co_{1.25}Al_{0.75}O_5$ [9]. The supercell in $Ca_2Co_{1.6}Ga_{0.4}O_5$ would then be $a = a_{BM}$, $b = b_{BM}$ and $c = 6a_{BM}$ (neglecting the streaking along the *b*-axis) compared to $a = a_{BM}$, $b = b_{BM}$ and $c = na_{BM}$ (n varies between different crystallites) in $Ca_2Co_{1.25}Al_{0.75}O_5$. This latter modulation has been shown to be caused by a variation of the relative orientation of the chains of tetrahedra running parallel to the *a*-axis in the *a*–*c* plane. The modulation along the *c*-axis in the *a*–*c* plane is also seen as streaking and weak superstructure reflections in the [110] SAED ZAP shown in Fig. 5 together with the corresponding HREM image. It can be seen that the crystallite consists of slabs normal to the *c* -axis. The width of these slabs varies, which gives rise to the streaking. We are not completely sure about the origin of this phenomenon. However, as the contrast and distances are more or less identical in the different slabs, one explanation could therefore be that they are alternating slabs of BM oriented along [1$\bar{1}$0] and [110].

Table 3
Selected interatomic distances and angles for $Ca_2Co_{1.6}Ga_{0.4}O_5$

Distances (Å)			Angles (°)		
Octahedron					
O1–Co1/Ga1	(×2)	1.880(5)	O1–Co1/Ga1–O1	(×2)	92.95
				(×2)	87.05
O1–Co1/Ga1	(×2)	1.974(5)			
O2–Co1/Ga1	(×2)	2.147(3)	O1–Co1/Ga1–O2	(×4)	87.40
				(×4)	92.60
Tetrahedron					
O2–Co2/Ga2	(×2)	1.808(4)	O2–Co2/Ga2–O2	(×2)	126.09
O3–Co2/Ga2	(×1)	1.923(8)	O2–Co2/Ga2–O3	(×2)	104.11
					107.96
O3–Co2/Ga2	(×1)	1.876(7)	O3–Co2/Ga2–O3		104.58
Calcium					
Ca–O3		2.310(5)			
O2		2.314(4)			
O1		2.429(7)			
		2.483(6)			
		2.536(7)			
O2		2.584(7)			
O1		2.643(6)			
O2		2.832(7)			
O2		3.307(5)			

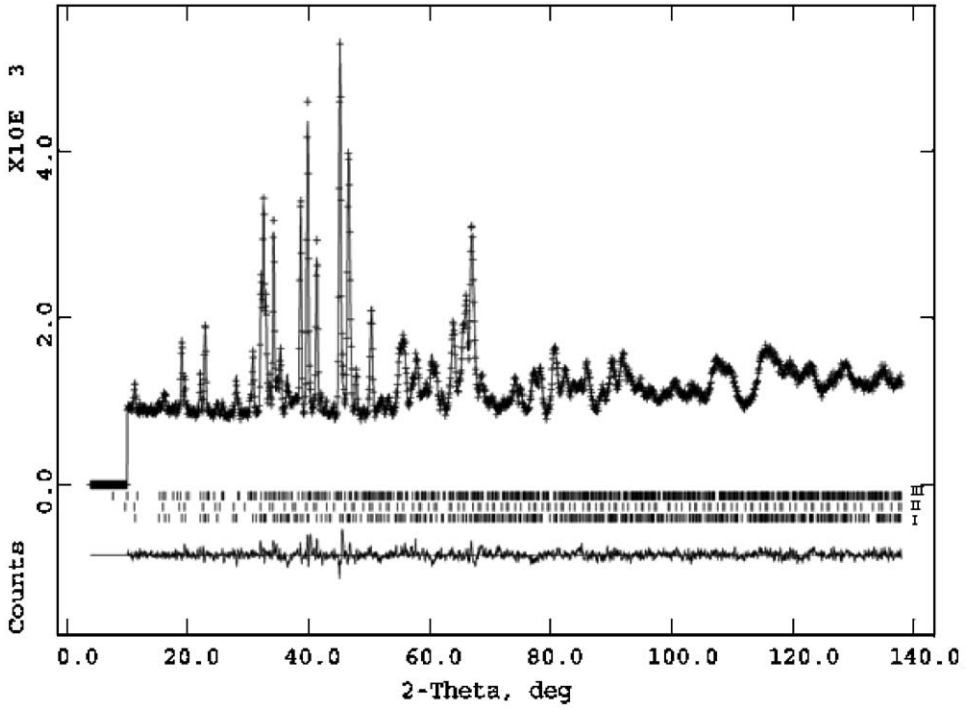

Fig. 2. Observed, calculated and difference neutron diffraction profiles for $Ca_2Co_{1.6}Ga_{0.4}O_5$ (I), $Ca_2Ga_{1.2}Co_{0.8}O_{4.8}$ (II) and $Ca_3Ga_4O_9$ (III).

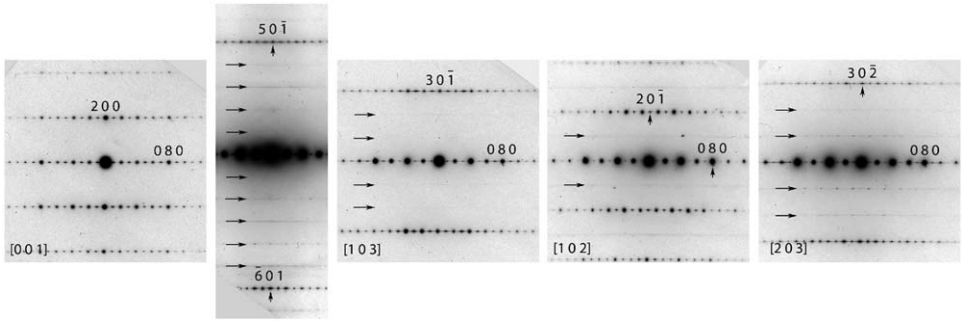

Fig. 3. Selected-area diffraction patterns of $Ca_2Co_{1.6}Ga_{0.4}O_5$ recorded during a rotation around the *b*-axis. There is streaking along the *b*-axis in all patterns. When leaving the [001] zone-axis orientation, extra lines appear at positions between the $0\,k\,0$ and $h\,0\,l$ reflections. These are marked with arrows. Note that the viewing direction of the second pattern from the left is halfway between the zone axes [105] and [106]. In the streaking along the *b*-axis at the positions between the $0\,k\,0$ and $h\,0\,l$ reflections, weak intensity maxima can be seen at $q = 1 \times \langle 010 \rangle_{BM}$, indicating that the preferred repeating sequence along the *b*-axis of the disordered structure is the same as in the average structure.

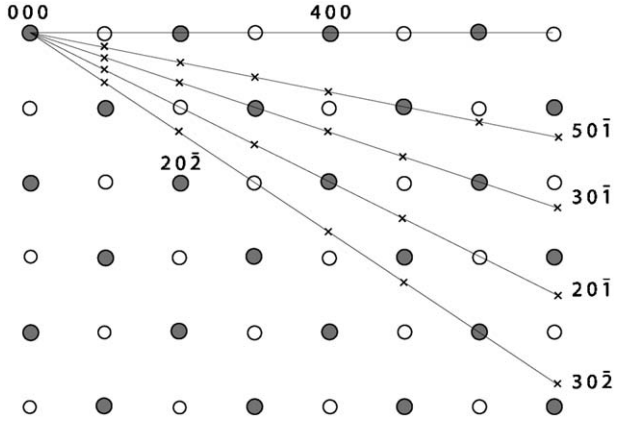

Fig. 4. Schematic drawing of the reciprocal lattice as viewed along [010]. The indexing corresponds to the BM-type cell. The empty and filled circles correspond to the BM and perovskite sublattice, respectively, and the crosses to the position of the diffuse lines in the SAED patterns shown in Fig. 3. The drawing shows that the extra lines in the [*u*0*w*] ZAPs in Fig. 3 should appear as streaking or superstructure reflections along the *c*-axis in the SAED patterns. The position of the extra lines can be explained by a modulation along the *c*-axis giving a supercell: $a = a_{BM}$, $b = b_{BM}$ and $c = 6 \times a_{BM}$ (neglecting the streaking along the *b*-axis).

The streaking along the *b*-axis then indicated disorder in the stacking sequence of the layers of tetrahedra. (Although the intensity maxima in the streaking at $q = 1 \times \langle 010 \rangle$ in the SAED [203] ZAP indicate that the preferred repeating distance is the same as in the average structure also for the modulated structure.) This disorder in the stacking sequence of the layers of tetrahedra can be seen in HREM images recorded along [001] as contrast variations (some marked with arrows), see Fig. 6. Such disorder is common, as reported by several researches, and is interpreted as intergrowth between slabs of *Pnma*- and *I*2*mb*-type BM [17]. The presence of *I*-centred BM in this compound is indicated by the [101] ZAP SAED patterns shown in Fig. 7a and b.

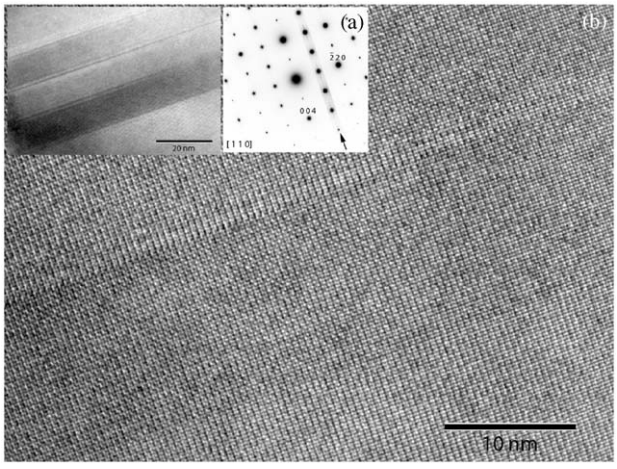

Fig. 5. SAED pattern of $Ca_2Co_{1.6}Ga_{0.4}O_5$ viewed along [110] with streaking (arrowed) along the *c*-axis (a). The corresponding HREM image (b) shows a structure consisting of alternating slabs. An overview with a smaller magnification is inserted in the HREM image.

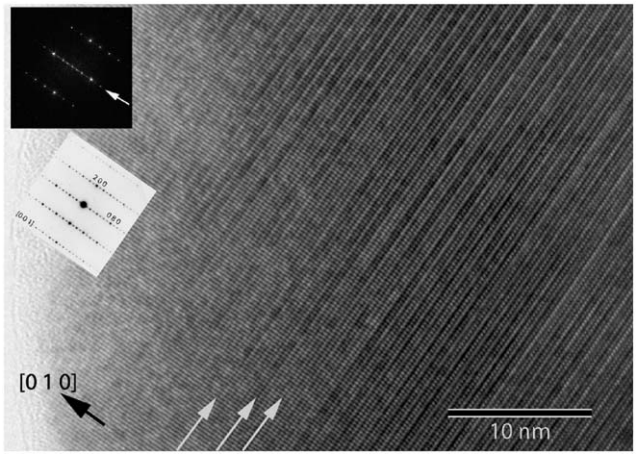

Fig. 6. HREM image of $Ca_2Co_{1.6}Ga_{0.4}O_5$ viewed along [001]. The SAED pattern corresponding to the crystallite and an FFT transform of the image are shown in the inset. The streaking in the FFT and SAED patterns can be seen as dark contrast variation in the HREM images. Three of these are marked with arrows.

They are from different areas of one single crystallite fragment with *Pnma*- and *I2mb*-type BM, respectively.

In compounds that crystallize in BM-type structure, often intergrowth between domains oriented along [100] and [001] is observed. This is also the case for $Ca_2Co_{1.6}Ga_{0.4}O_5$. An HREM image showing this is seen in Fig. 8. This is not surprising, because the domains have the [110] direction in the perovskite sublattice in common. The shift in direction can easily be obtained by rotating the tetrahedra around the *b*-axis.

In the crystal structure of $Ca_2Co_{1.6}Ga_{0.4}O_5$, the cobalt atoms are located predominantly in octahedral positions while both cobalt and gallium atoms are found in the tetrahedral ones. This is very similar to the situation reported for the Sr analogue [7]. The CoO_6 octahedron is highly distorted, with equatorial Co–O distances from 1.880(5) to 1.974(5) Å and axial distances 2.147(3) Å. (The O–Co1–O bond angles within the octahedra are close to 90°.) Such a highly distorted octahedron is normally observed for calcium-containing BMs, e.g. Ca_2MnGaO_5 [17], because the small ionic radius of Ca^{2+} leads to tilting of the MO_6 octahedron and concomitant distortion of the layers of octahedra.

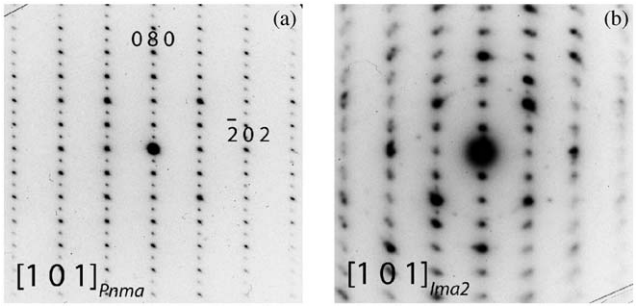

Fig. 7. Two SAED patterns from different domains found in a crystallite oriented along $\langle 100 \rangle_p$ (perovskite): (a) a [101] SAED ZAP indicating a *Pnma*-type BM structure and (b) a [101] SAED ZAP indicating an *I2mb*-type BM structure.

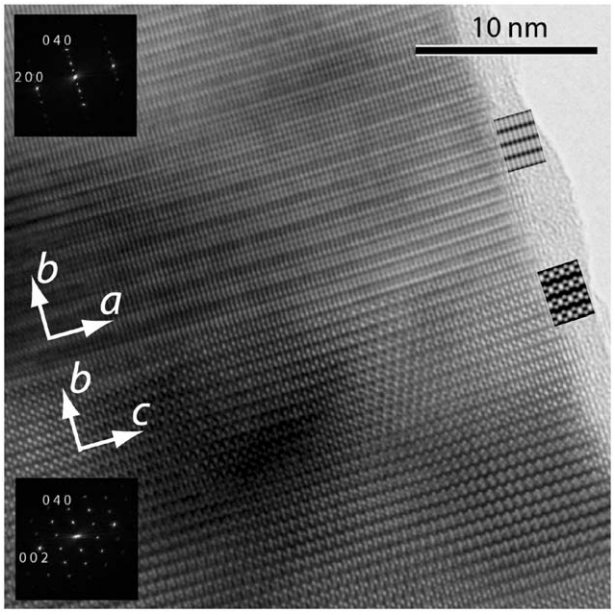

Fig. 8. HREM image of $Ca_2Co_{1.6}Ga_{0.4}O_5$ viewed along $\langle 110 \rangle_p$ (p-perovskite subcell). The area shown consists of two intergrown BM domains viewed along [100] and [001]. An FFT of each domain is inserted, as well as simulated HREM images (crystal thickness = 40 Å, defocus = −400 Å), using the coordinates in Table 2.

The valence of the atoms calculated from the bond valence formalism [18], using the bond lengths in Table 3 are all reasonable: Ca = 2.0, Co1/Ga1 = 2.7, Co2/Ga2 = 2.8, O1 = 2.0, O2 = 1.8 and O3 = 2.0. The values for Co/Ga are close to 3.0, which is the oxidation number according to the composition obtained from the Rietveld refinement.

There are several distinct differences between $Ca_2Co_{1.6}Ga_{0.4}O_5$ and the recently reported BM-type $Sr_2Co_{2-x}Ga_xO_5$, $0.3 \leqslant x \leqslant 0.8$ [7]. The first one is that the calcium-contained BM phase seems to have nearly no homogeneity range, while that of the strontium analogue $Sr_2Co_{2-x}Ga_xO_5$ is quite wide, $0.3 \leqslant x \leqslant 0.8$. It has to be noted that $Sr_2Co_2O_5$ [5,6] also crystallizes in BM structure, while $Ca_2Co_2O_5$, which can be prepared by low-temperature decomposition of carbonates does not form this structure [19]. No refined crystal structure is available for this compound, although it has been suggested to have a perovskite-related structure with an oxygen vacancy ordering different from that in BM. We have not been able to confirm the existence of this compound. All attempts to synthesize it via a ceramic route lead to the formation of $Ca_3Co_2O_6$ and Co_3O_4. A second difference between $Ca_2Co_{1.6}Ga_{0.4}O_5$ and its strontium analogue is that a BM structure with visible preferential ordering of the chains of tetrahedra in adjacent layers forms in the first case. The reason for this could be the lower synthesis temperature and/or that the smaller calcium stabilizes the ordered variant of the BM structure with out-of-phase type ordering of the chains in adjacent layers (space group *Pnma*), e.g. $Ca_2Fe_2O_5$ [1,2], Ca_2FeGaO_5 [20], $Ca_2Fe_{2-x}Al_xO_5$, $x < 0.66$ [21,22] and Ca_2MnGaO_5 [17]. However, the TEM studies discussed above show that in $Ca_2Co_{1.6}Ga_{0.4}O_5$ the preference for the out-of-phase ordering is rather weak, since streaking and contrast variations due to disorder are frequently found in the ED patterns and the HREM images. One can assume that preferred formation of one of the ordered types of the BM structure depends on preparation route and heat treatments of the samples.

$Sr_2Co_{2-x}Ga_xO_5$ [7] and $Ca_2Co_{1.6}Ga_{0.4}O_5$ are both antiferromagnetic, with G-type ordering of the magnetic moments. In both structures, the magnetic moments of the cobalt atoms are directed along the chains of tetrahedra in the structure (Fig. 9).

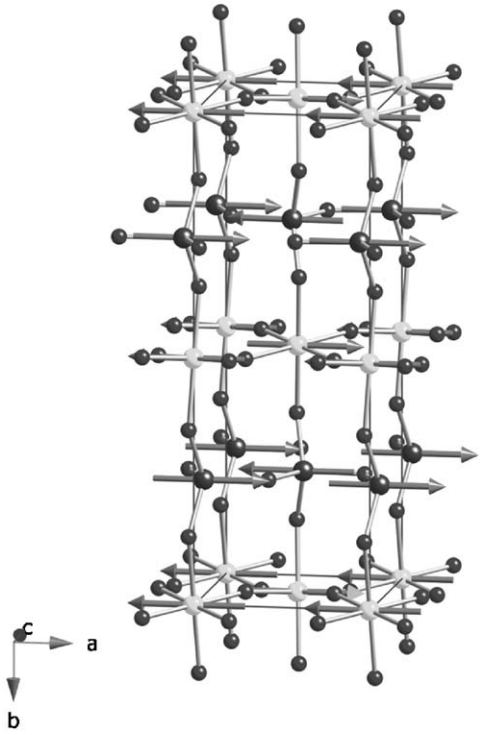

Fig. 9. Magnetic structure of $Ca_2Co_{1.6}Ga_{0.4}O_5$.

Acknowledgments

The authors thank Mr. H. Rundlöf for the neutron diffraction experiment. This research was partly supported by The Swedish Research Council, The Royal Swedish Academy of Sciences (KVA) and the Russian Foundation for Basic Research (grant ♯02-03-32990). Acknowledgment is made to the donors of the American Chemical Society Petroleum Research Fund (PRF ACS 38459-AC5). S.Ya.I. is grateful to the Scientific Council of MSU.

References

[1] A.A. Colville, Acta Cryst. B 26 (1970) 1469.
[2] P. Berastegui, S.-G. Eriksson, S. Hull, Mater. Res. Bull. 34 (1999) 303.
[3] J. Berggren, Acta Chem. Scand. 25 (1971) 3616.
[4] M. Schmidt, S.J. Campbell, J. Solid State Chem. 156 (1999) 292.
[5] T. Takeda, Y. Yamaguchi, H. Watanabe, J. Phys. Soc. Jpn. 33 (1972) 970.
[6] J.-C. Grenier, S. Ghobane, G. Demazeau, M. Pouchard, P. Hagenmuller, Mater. Res. Bull. 14 (1979) 831.
[7] F. Lindberg, S.Ya. Istomin, P. Berastegui, G. Svensson, S.M. Kazakov, E.V. Antipov, J. Solid State Chem. 173 (2003) 395.
[8] F. Lindberg, G. Svensson, S.Ya. Istomin, S.V. Aleshinskaya, E.V. Antipov, J. Solid State Chem. 177 (2004) 1592.
[9] S. Lambert, H. Leligny, D. Grebille, D. Pelloquin, B. Raveau, Chem. Mater. 14 (2002) 1818.
[10] S.Ya. Istomin, E.V. Antipov, G. Svensson, J.P. Attfield, V.L. Kozhevnikov, I.A. Leonidov, M.V. Patrakeev, E.B. Mitberg, J. Solid State Chem. 167 (2002) 196.
[11] J. Grins, S.Ya. Istomin, G. Svensson, to be published elsewhere.
[12] V.D. Barbanyagre, T.I. Timoshenko, A.M. Ilyinets, V.M. Shamshurov, Powder Diff. 12 (1997) 22.
[13] A.C. Larson, R.B. Von Dreele, General Structure Analysis System (GSAS), Los Alamos National Laboratory Report LAUR 86-748, 2000.
[14] Roar Kilaas, MacTempas, www.totalresolution.com.
[15] A.R. Schulze, H. Mueller-Buschbaum, Monatsh. Chem. 112 (1981) 149.
[16] A.M. Abakumov, M.G. Rozova, B.Ph. Pavlyuk, M.V. Lobanov, E.V. Antipov, O.I. Lebedev, G. Van Tendeloo, O.L. Ignatchik, E.A. Ovtchenkov, Yu.A. Koksharov, A.N. Vasil'ev, J. Solid State Chem. 160 (2001) 353.
[17] A.M. Abakumov, M.G. Rozova, B.Ph. Pavlyuk, M.V. Lobanov, E.V. Antipov, O.I. Lebedev, G. Van Tendeloo, D.V. Sheptyakov, A.M. Balagurov, F. Bouree, J. Solid State Chem. 158 (2001) 100.
[18] I.D. Brown, D. Altermatt, Acta Cryst. B 41 (1985) 244.
[19] K. Vidyasagar, J. Gopalakrishnan, C.N.R. Rao, Inorg. Chem. 23 (1984) 1206.
[20] R. Arpe, R. von Schenk, H. Mueller-Buschbaum, Z. Anorg. Allg. Chem. 410 (1974) 97.
[21] D.K. Smith, Acta Cryst. 15 (1962) 1146.
[22] S. Geller, R.W. Grant, L.D. Fuller, J. Phys. Chem. Solids 31 (1970) 793.